www.czasopisma.pan.pl PAN www.journals.pan.pl
Chemical and Process Engineering 2018, 39 (2), 185–196
DOI: 10.24425/119108

MEMBRANE FOULING IN THE ULTRAFILTRATION OF WATER–PROTEIN–SODIUM CHLORIDE MODEL SYSTEMS

Konrad Ćwirko[1*], Elwira Tomczak[2], Daniela Szaniawska[3]

[1] Maritime University of Szczecin, Faculty of Mechanics,
Waly Chrobrego Str. 1-2, 70-500 Szczecin, Poland

[2] Lodz University of Technology, Faculty of Process and Environmental Engineering,
Wolczanska 213, 90-924 Lodz, Poland

[3] Maritime University of Szczecin, Faculty of Economics and Transport Engineering,
H. Poboznego 11, 70-507 Szczecin, Poland

This paper presents ultrafiltration results of model BSA (bovine serum albumin) and MB (myoglobin) solutions prepared with or without NaCl addition. The protein concentrations in the solutions were equal to 0.05 g·dm^{-3} for MB and 0.5 g·dm^{-3} for BSA. The ultrafiltration tests were performed using a laboratory scale unit equipped with 90 mm ceramic disc membranes with a filtration area of 5.6×10^{-3} m^2 and cut-off of 50 or 150 kDa. The tests were run under constant process conditions, i.e. a cross flow volume (*CFV*) of 5 m·s^{-1}, transmembrane pressure (*TMP*) of 0.2 MPa, temperature of 20 °C and NaCl concentration of 0 or 10 wt%. The installation worked in a semi-open mode with a continuous permeate discharge and retentate recycle. The performance of the membranes was measured with the permeate volumetric flow rate, J_V (m^{3}m^{-2}s^{-1}) while their selectivity was determined by the protein rejection, R. The paper evaluates and discusses the protein rejection mechanisms as well as the influence of the membrane cut-off and sodium chloride concentration in the feed on the flux decline during the ultrafiltration of BSA and MB. Moreover, it provides an analysis of the first fouling phase by applying usual filtration laws.

Keywords: ultrafiltration, ceramic membranes, fouling models, BSA, myoglobin

1. INTRODUCTION

Recently, pressure-driven membrane processes have gained importance in biotechnology, environmental engineering and other areas of human activity. The significance of membrane techniques, especially in concentrating proteins via ultrafiltration, comes from their ability for highly effcient size and/or charge based protein separation. In order to meet the industrial requirements for protein separation, ultrafiltration technology is still being modified for the purposes of developing advanced techniques with low membrane fouling, high permeation fluxes and high selectivity. The separation performed using charged ultrafiltration membranes is a promising technology for the concentration and fractionation of proteins with different molecular weights. In the separation processes employing charged *UF* membranes, both size and charge based exclusion are involved. Thus, the efficiency of separation is strongly dependent on such operating parameters as pH, salt concentration and system hydrodynamics (Saxena et al., 2009).

Ehsani and Nystrom (1995) studied charged ultrafiltration membranes and separated enzymes from a fermentation broth and myoglobin from BSA. They achieved high efficiency of the separation for the

* Corresponding author, e-mail: k.cwirko@am.szczecin.pl

smaller protein at its IEP. Zydney et al. (2003) studied electrostatic interactions between charged proteins and charged membranes and showed that pH and ionic strength had strong effects on the separation effects. Moreover, Lee et al. (2011) showed that the fouling behavior of positively (Lys) and negatively charged (BSA) proteins was observed in a positively charged MWCNT membrane together with high sensitivity to the pH and ionic strength of the feed solution. The permeation flux through the MWCNT membrane was found to be strongly influenced by pH and ionic strength in a single protein filtration test. Recently, Almecija et al. (2007) have been focusing on the effect of pH on the fractionation of BSA and other proteins and found that higher permeation fluxes and better protein separation occured at extreme pH levels, including the lowest pH levels. Furthermore, de la Casa et al. (2007) studied the influence of pH and salt concentration on the MF cross flow of BSA through a ceramic membrane. Results revealed that the highest protein transmission was obtained at the isoelectric point of BSA (pH 4.9) and that the addition of salt resulted in higher protein transmission and a higher permeate flow rate.

Ultrafiltration was traditionally performed using polymeric membranes (Shah et al., 2007). However, polymeric membranes are susceptible to chemical degradation by strong alkaline or acidic solutions, significantly reducing the membrane lifetime. In addition, some polymeric membranes have limited mechanical stability, leading to a reduction in permeability under high pressures and a possible membrane failure. These membranes are also inappropriate for steam sterilization because they increase the overall biological ballast in subsequent processing steps (Saxena et al., 2009).

The above mentioned limitations have inspired the development of a variety of inorganic *UF* membranes exhibiting greatly enhanced chemical, thermal and mechanical stability (Lim and Bai, 2003). However, such membranes appear to have several drawbacks in treating the feed water containing effluent organic matter (such as proteins) and to be susceptible to fouling (Lee et al., 2016; Mohammadi et al., 2003).

In general, membrane fouling can be described as a reduction in membrane permeability as a result of the flow resistance appearing due to pore blocking, concentration polarization and cake formation (Abdelrasoul et al., 2015; Fang, 2013; US EPA, 2005). Membrane permeability declines due to the cumulation of foulants on the membrane surface or within the membrane pores (Dabestani et al., 2017; Gkotsis et al., 2014). Serious membrane fouling is often caused by foulants alone, such as BSA or other mixtures of proteins (Luján-Facundo et al., 2015; Ma et al., 2015). Moreover, Almecija et al. (2007) showed that the fouling mechanism depends mainly on the electrostatic interactions between proteins but also between a protein and the membrane.

On the other hand, the long term effects of membrane fouling may lead to irreversible blockage of the membrane and a reduction in the membrane lifetime (Brião et al., 2012; Cheng et al., 2001; Cinta et al., 2008). To maintain the technical and economic viability of a membrane process, membrane fouling should be kept to a minimum (Lieu Le and Nunes, 2016).

The purpose of this paper was to investigate the permeability of ceramic membranes with a molecular weight cut-off of 50 or 150 kDa in the ultrafiltration of water–protein–sodium chloride systems with regard to the resistance-in-series model and typical fouling mechanisms.

2. THEORY

In general, during ultrafiltration of a liquid mixture, the permeation flux increases with increasing transmembrane pressure. According to Wiesner et al. (1992), the permeation flux of particle-free water across a clean membrane can be determined with Darcy's law given by Eq. (1):

$$J_W = \frac{TMP}{\mu \cdot R_M} \tag{1}$$

During ultrafiltration of a solution under constant pressure, the permeation flux can be calculated with the resistance-in-series model (Eq. (2)):

$$J_V = \frac{TMP}{\mu \cdot R_T} \tag{2}$$

Thus, the total resistance R_T in a membrane system is the sum of the membrane and the fouling resistances (Eq. (3)):

$$R_T = R_M + R_F \tag{3}$$

These resistances can be calculated from permeation flux data J_V and from the clean water flux through a clean membrane J_W.

Hermia's models are the most useful for a detailed description of the flux decline in cross-flow ultrafiltration. These models can be expressed as simple linear equations relating the permeation flux J_V and time t to the filtration constants of each model K_m, K_p, K_c and the initial permeation flux J_0. The initial flux depends mainly on the membrane resistance R_M and deteriorates over time as a result of membrane fouling. The mechanisms of membrane fouling usually include pore blocking and cake formation. Thus, the flux in the ultrafiltration process can be determined based on the membrane resistance R_M, the pore blocking resistance $R_p$and the cake resistance R_c. The sum of these resistances corresponds to the total resistance R_T.

The permeation flux resulting from the membrane resistance (Wiesner et al., 1992) can be expressed in the linearized form as in Eq. (4):

$$\frac{1}{J_V} = \frac{1}{J_0} + K_m \cdot t \tag{4}$$

When the ultrafiltration process is limited by the pore blocking mechanism, Eq. (4) takes the form of Eq. (5):

$$\ln J_V = \ln J_0 - K_P \cdot t \tag{5}$$

In the case of cake formation, the linearized form is given by Eq. (6):

$$\frac{1}{J_V^2} = \frac{1}{J_0^2} + K_C \cdot t \tag{6}$$

Fitting the experimental data to Eqs. (4)–(6) allows to recognize the mechanism of membrane fouling and to determine the filtration constants. The rejection coefficient R, being a measure of the membrane selectivity, can be calculated from Eq. (7):

$$R = 1 - \frac{C_P}{C_F} \tag{7}$$

3. EXPERIMENTAL

The test runs were performed using a laboratory scale Spirlab unit (Fig. 1) equipped with ceramic membranes (90 mm in diameter) provided by TAMI.

During each ultrafiltration test samples of the feed F and the permeate P were collected. In each run the feed volume was kept constant (1 dm^3). The protein concentrations in the feed were equal to 0.05 g/dm^3 for myoglobin solutions and 0.5 g/dm^3 for BSA solutions, as summarized in Table 1.

The membrane unit worked in semi-open mode with the retentate recycle and partial removal of the permeate. The process was conducted under constant conditions: $TMP = 0.2$ MPa, $CFV =$ of 5 $m \cdot s^{-1}$ and temperature = 20 °C. The experiments were performed at pH = 7.1 (0% NaCl) or pH = 8.2 (10% NaCl). In each test, permeate samples were collected after 60 minutes to determine the protein content. The feed

Fig. 1. Laboratory UF unit with ceramic membranes

Table 1. Characteristics of used proteins and tested ceramic membranes

Protein	Protein molecular weight, *MW*, (kDa) and isoelectric point, IEP	Protein concentration in the feed, C_F ($g \cdot dm^{-3}$)	Membrane cut-off, *MWCO*, (kDa) and point of zero charge, PZE	Water permeate through clean membrane, J_W ($m^3 m^{-2} s^{-1}$)	Resistance of clean membrane, R_M (m^{-1})
BSA	69 4.9	0.5	50/150/6.9	6.8×10^{-5}	2.94×10^{12}
MG	17 7.0	0.05	50/150/6.9	11.8×10^{-5}	1.70×10^{12}

and the permeate samples were analyzed with a UV–VIS HITACHI U-501 spectrometer in order to calculate the protein rejection (Eq. (7)). The permeation flux J_V was calculated from the permeate volume V_P measured over time t. The duration of each ultrafiltration run was set to 60 minutes. After each run, the membrane module and the *UF* unit were chemically cleaned, according to the procedure recommended by the manufacturer. The cleaning process was carried out until the membrane reached the hydraulic permeability characteristic of a clean membrane (Table 1).

4. RESULTS AND DISCUSSION

4.1. Ultrafiltration process in view of the resistance-in-series model

The ultrafiltration tests were carried out under constant operating conditions ($TMP = 0.2$ MPa, $CFV = 5\ m \cdot s^{-1}$, temperature $= 20\ ^\circ C$) using two different sodium chloride concentrations in the feed, i.e. 0 wt%

(pH = 7.1 ± 0.4) or 10 wt% (pH = 8.2 ± 0.4). The results including the permeation flux J_V and the protein rejection R are shown in Table 2.

Table 2. Experimental and calculated results of model protein solutions under constant operating conditions (TMP = 0.2 MPa, CFV = 5 m·s^{-1}, temperature = 20 °C)

Protein concentration, C_F g·dm^{-3}/membrane, $MWCO$, kDa	NaCl (wt.%)	UF time, t (s)	Permeate flux $J_V \times 10^{-5}$ (m^{3}m^{-2}s^{-1})	R (–)	pH	$R_T \times 10^{12}$ (m^{-1})	$R_F \times 10^{12}$ (m^{-1})	R_T/R_F (%)
	0	0	11.8		7.1 ± 0.4	1.7	0	–
		600	1.7			11.76	10.6	85.5
0.5 g BSA dm^{-3}		3600	1.5	0.99		13.3	11.6	83.2
/150 kDa	10	0	11.8		8.2 ± 0.4	1.7	0	–
		600	1.4			14.58	12.88	88.3
		3600	1.2	0.93		16.7	15.5	92.8
	0	0	6.8		7.1 ± 0.4	2.94	0	–
		600	2.3			8.69	5.75	66.2
0.5 g BSA dm^{-3}		3600	2.1	0.84		9.52	6.58	69.1
/50 kDa	10	0	6.8		8.2 ± 0.4	2.94	0	–
		600	1.8			11.1	8.16	73.5
		3600	1.5	0.80		13.3	10.36	77.9
	0	0	11.8		7.1 ± 0.4	1.7	0	–
		600	8.8			2.27	0.57	25.1
0.05 g MG dm^{-3}		3600	8.0	0.21		2.5	0.8	32.0
/150 kDa	10	0	11.8		8.2 ± 0.4	1.7	0	–
		600	5.6			3.57	1.87	52.4
		3600	5.0	0.39		4.0	2.3	57.5
	0	0	6.8		7.1 ± 0.4	2.94	0	–
		600	1.5			13.3	10.36	77.9
0.5 g MG dm^{-3}		3600	1.0	0.95		20.0	17.06	85.3
/50 kDa	10	0	6.8		8.2 ± 0.4	2.94	0	–
		600	4.0			5.0	2.6	41.2
		3600	3.5	0.59		5.71	2.77	48.5

As can be seen from Table 2, the highest protein rejection $R = 0.99$ was achieved during the ultrafiltration of the BSA solution containing no salt. When the BSA solution contained 10% NaCl, the BSA rejection decreased to $R = 0.93$. It was caused by the membrane–BSA–NaCl interaction (Kuca and Szaniawska, 2009). At a pH of 7.1 and 8.2, greater than the isoelectric point of BSA (4.9) and the point of zero charge (6.9), both the protein and the membrane were negatively charged. A decrease in the protein rejection in the presence of Na^+ ions was a result of neutralization of the membrane and the BSA molecule charge. The lowest myoglobin rejection was observed in the ultrafiltration process performed with a ceramic 150 kDa membrane. Considering only the molecular weight of myoglobin, such behavior of the membrane can be attributed to the large difference between the protein molecular weight and the membrane cut-off (17 and 150 kDa, respectively). The data presented in Table 2 show a flux decline during the ultrafiltration of both protein solutions (BSA and MB). The permeation flux J_V reached the highest level at the beginning of each run and decreased over time as visible in Fig. 2. It was observed that a sharp flux decline occurred during the first 10 minutes of the experiment. Then, the flux stayed at a pseudo-steady state level until the end of the run. It indicates that fouling of the membrane occurred rapidly once the ultrafiltration process had been started.

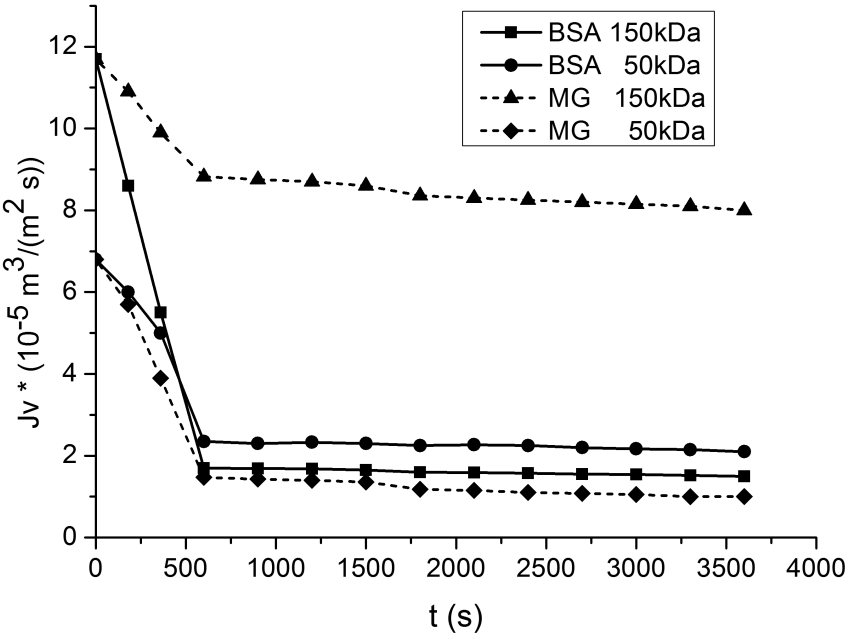

Fig. 2. Permeation flux vs. time during the ultrafiltration of model BSA and MB solutions for membranes with different cut-offs ($CFV = 5$ m·s^{-1}; $TMP = 0.2 \times 10^6$ Pa; 0% NaCl)

Permeability of the tested membranes was dependent on the membrane cut-off and the presence of sodium chloride in the feed. On the one hand, permeability of the membrane with a 150 kDa cut-off was higher than that of the membrane with a 50 kDa cut-off. On the other hand, the permeability was lower when the feed contained sodium chloride in addition to the protein. These results are similar to the data obtained earlier by Kuca and Szaniawska (2009) and the data reported in other studies (Casa et al., 2007; Zulkali et al., 2005). The total resistance of both tested membranes for both separated proteins is shown in Fig. 3 as a function of time. It was observed that the greatest increase in total resistance caused by fouling also took place during the first 10 minutes. In the case of MB solution and 150 kDa membrane (Fig. 3),

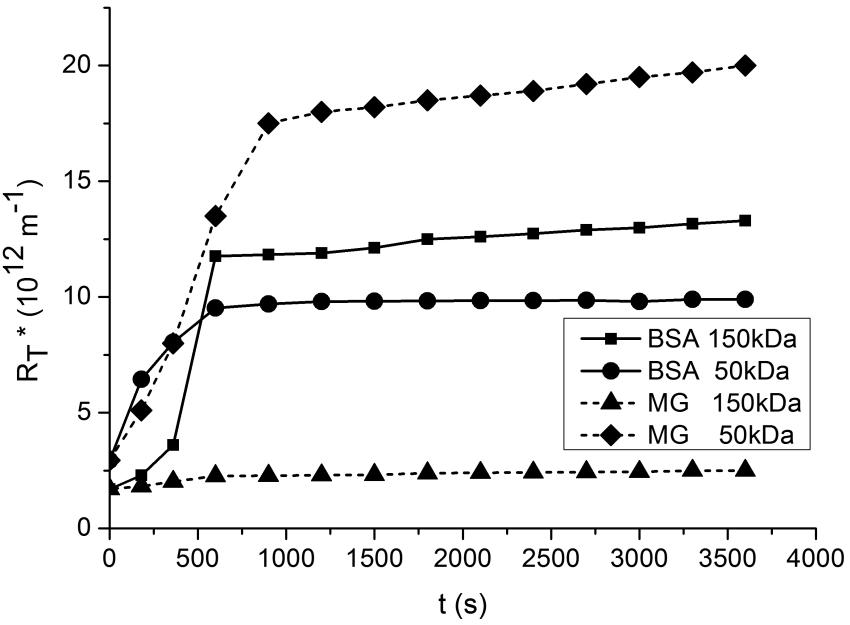

Fig. 3. Total resistance R_T vs. time during the ultrafiltration of model BSA and MB solutions for membranes with different cut-offs ($CFV = 5$ m·s^{-1}; $TMP = 0.2 \times 10^6$ Pa; 0% NaCl)

the increase in total resistance during the first 10 minutes was much less evident because the whole process was limited both by fouling and the membrane itself.

The analysis of the experimental data in view of the resistance-in-series model shows that the ultrafiltration of BSA ($MW = 69$ kDa) with the membrane having a 150 kDa cut-off was significantly limited by the fouling resistance (Fig. 4.), as the R_F/R_T ratio ranges from 83.2 to 92.8%. In the case of *MB,* having a lower molecular weight (17 kDa), the R_F/R_T ratio ranges from 25.1 to 57.5% (Table 2), indicating that the *UF* process was limited by both the membrane and the fouling resistances (Figs. 4, 5).

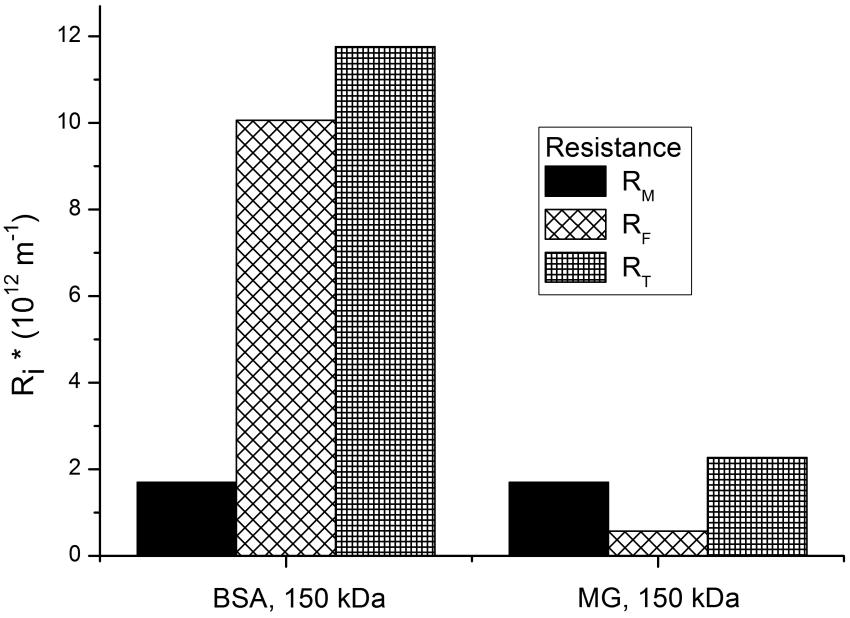

Fig. 4. Comparison of transfer resistances R_M, R_T, R_F during the ultrafiltration of model BSA and MB solutions with a membrane having a 150 kDa cut-off (0% NaCl; $CFV = 5\ m{\cdot}s^{-1}$; $TMP = 0.2 \times 10^6$ Pa)

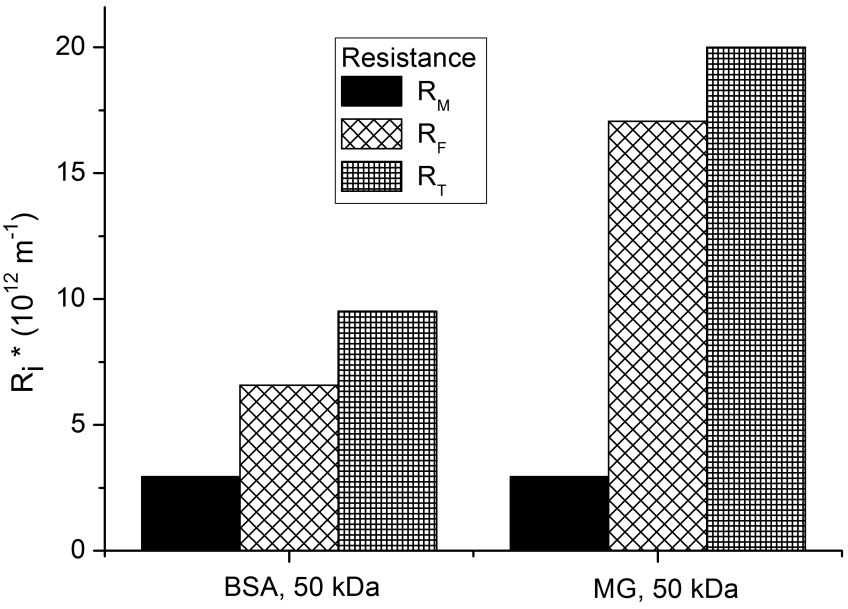

Fig. 5. Comparison of transfer resistances R_M, R_T, R_F during the ultrafiltration of model BSA and MB solutions with a membrane having a 50 kDa cut-off (0% NaCl; $CFV = 5\ m{\cdot}s^{-1}$; $TMP = 0.2 \times 10^6$ Pa)

4.2. Assessment of the fouling mechanism

The experimental data presented in Fig. 2 indicate that fouling of the membranes occurred during the initial 10 minutes of the process. Then, a pseudo-steady state was reached. For this reason, in order to identify the existing fouling mechanisms the experimental ultrafiltration values of the permeation flux recorded during the first 10 minutes were fitted to typical fouling models (Eqs. (4)–(6)). The results of data fitting are presented in Figs. 6–8. The values of the estimated model constants (K_m, K_p, K_c) along with the determination coefficients (R^2) are summarized in Table 3.

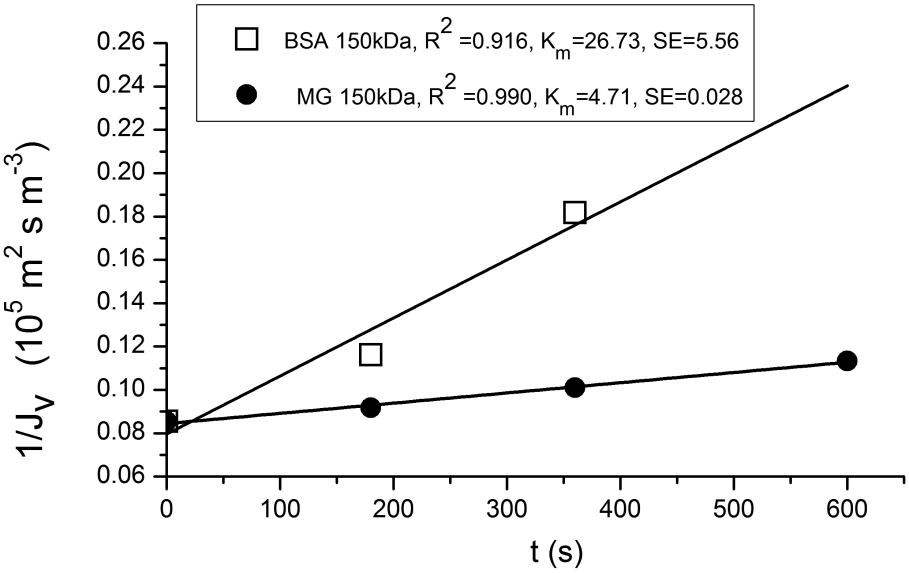

Fig. 6. The results of fitting experimental data to the membrane resistance model (Eq. (4))

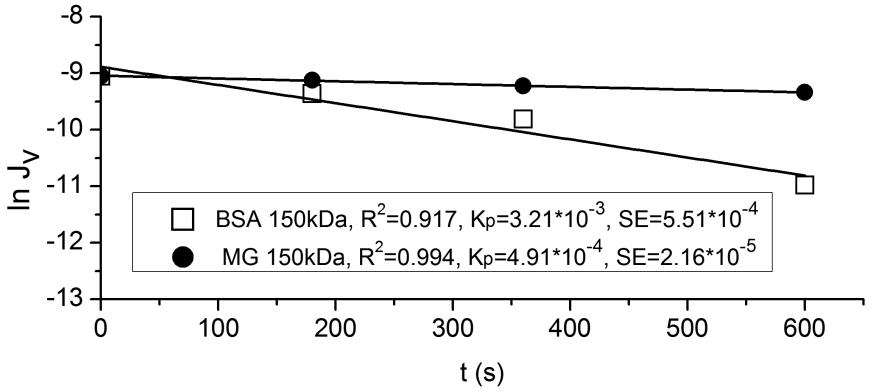

Fig. 7. The results of fitting experimental data to the pore blocking resistance model (Eq. (5))

Figures 6–8 show comparisons between the experimental data and the results predicted with the accepted resistance models. The filtration constants K_m, K_p, K_c and the determination coefficient R^2 calculated for these models imply that the membrane fouling mechanism follows chiefly the cake formation model. As can be seen from Table 3, the values of R^2 obtained for the other two models are noticeably lower. For the cake resistance model, R^2 varies from approximately 0.808 to 0.999, while the K_c values range from 9.38×10^4 m^{-1} to 1.21×10^7 m^{-1}. The second most accurate model is the pore blocking model (R^2 in a range of 0.875 to 0.994), followed by the membrane resistance model (R^2 in a range of 0.740 to 0.990). However, the pore blocking model and the cake resistance model both give good results with regard to the flux decline over time during the ultrafiltration of MB without the NaCl addition, when the membrane

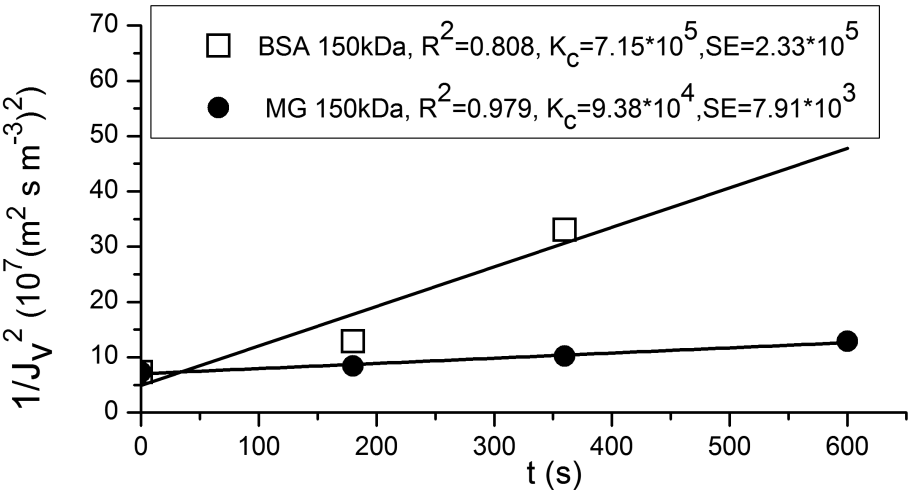

Fig. 8. The results of fitting experimental data to the cake formation resistance model (Eq. (6))

Table 3. Summary of the constants of filtration resistance models (Eq. (4)–(6)) and determination coefficients R^2

Protein	Membrane Cut-off (kDa)	NaCl conc. in feed, (wt. %)	Membrane resistance – limited model		Pore blocking resistance – limited model		Cake formation resistance – limited model	
			K_m (m^{-1})	R^2	K_p (s^{-1})	R^2	K_c ($s \cdot m^{-2}$)	R^2
Bovine serum albumin, BSA	150	0	26.73	0.916	3.21×10^{-3}	0.917	7.15×10^5	0.808
		10	139.54	0.745	4.12×10^{-3}	0.910	1.21×10^7	0.955
	50	0	59.50	0.788	2.20×10^{-3}	0.875	2.15×10^6	0.992
		10	88.10	0.740	2.62×10^{-3}	0.905	6.63×10^6	0.996
Myoglobin, MG	150	0	4.71	0.990	4.91×10^{-4}	0.994	9.38×10^4	0.979
		10	15.87	0.885	1.40×10^{-3}	0.970	5.29×10^5	0.999
	50	0	119.0	0.788	3.20×10^{-3}	0.910	9.95×10^6	0.994
		10	18.47	0.860	8.81×10^{-4}	0.925	7.88×10^5	0.989

with a cut-off of 150 kDa is used. In this case, the molecular weight of MB is much lower than the *MWCO* of the membrane. Therefore, the protein particles can enter and clog the membrane pores and then form a cake on the membrane surface.

5. CONCLUSIONS

This paper focuses on the behavior of laboratory-scale ceramic ultrafiltration membranes (with molecular weight cut-offs of 50 and 150 kDa) during the separation of BSA and MB. In the study, the protein solutions were prepared with or without sodium chloride addition. The experimental data were examined using the resistance-in-series model and the modified Hermia model.

Under constant process conditions, i.e. *TMP* (0.2 MPa), *CFV* (5 $m \cdot s^{-1}$) and temperature (20 °C), permeability and selectivity of the investigated membranes were dependent on the membrane cut-off, protein molecular weight and NaCl concentration. At a pH equal to 7.1 and 8.2, i.e. above the point of zero charge

and the isoelectric point of both proteins, permeability of the membranes decreased with increasing NaCl concentration in the feed. This tendency might have resulted from membrane fouling caused by the deposition of uncharged protein molecules onto the membrane surface. The calculated protein rejection was greater for BSA in comparison with MB having a lower molecular weight. The ultrafiltration tests revealed that the first 10 minutes of each experiment were crucial for the flux decline resulting from fouling of the membranes caused by the proteins. The application of the resistance-in-series model indicated that the fouling resistance R_F had a major influence on the flux decline during the separation of BSA with both membranes. A similar mechanism was observed when MB was separated with the membrane having a 50 kDa cut-off. However, it was noticed that the ultrafiltration of MB with the membrane having a 150 kDa cut-off was membrane resistance – limited.

The analysis of the membrane fouling mechanism based on the modified Hermia model showed that the best approximation of the experimental data was achieved when the cake resistance model was used, as evidenced by the highest value of R^2. The cake formation mechanism consists in the retention of substances having molecular weights larger than the membrane *MWCO*. On the other hand, pore blocking is caused by substances having molecular weights similar to the membrane *MWCO*. It means that fouling in the tested membranes was caused by the protein aggregates.

Since fouling in membrane systems is a complex problem, further studies are needed. This study, however, provides a framework for investigating the mass transfer resistance of ceramic ultrafiltration membranes having greater filtration areas.

SYMBOLS

CFV	cross flow velocity, $m \cdot s^{-1}$
C_F	solute (protein) concentration in the feed, $g \cdot dm^{-3}$
C_P	solute (protein) concentration in the permeate, $g \cdot dm^{-3}$
J_0	initial permeation flux, $m^3 m^{-2} s^{-1}$
J_W	water flux, $m^3 m^{-2} s^{-1}$
J_V	permeation flux through the ultrafiltration membrane, $m^3 m^{-2} s^{-1}$
K_c	parameter in the cake formation resistance model, $s \cdot m^{-2}$ (Eq. (6))
K_m	parameter in the membrane resistance model, m^{-1} (Eq. (4))
K_p	parameter in the pore blocking resistance model, s^{-1} (Eq. (5))
MW	solute (protein) molecular weight, kDa
MWCO	molecular weight cut-off, kDa
R	retention (Eq. (7))
R^2	determination coefficient
R_c	cake formation resistance, m^{-1} (Eq. (6))
R_F	fouling resistance, m^{-1} (Eq. (3))
R_M	membrane resistance, m^{-1} (Eq. (1))
R_p	pore blocking resistance, m^{-1} (Eq. (5))
R_T	total mass transfer resistance, m^{-1} (Eq. (2), (3))
t	ultrafiltration process time, s
TMP	transmembrane pressure, Pa
UF	ultrafiltration
UV–VIS	ultraviolet-visible
V_p	permeate volume, m^3

Greek symbols

μ	absolute viscosity of water, Pa s

Abbreviations

BSA	bovine serum albumin
F	feed
IEP	protein isoelectric point
Lys	lysine
MB	myoglobin
MWCNT	multi-walled carbon nanotube
P	permeate
PZE	membrane point of zero charge
SE	standard error

Research has been financed under the grants of the Ministry of Science and Higher Education no 3/S/IIT/14 and no 2/S/KFiCh/14

REFERENCES

Abdelrasoul A., Doan H., Lohi A., Cheng C.H., 2015. Mass transfer mechanisms and transport resistances in membrane separation process, In: Solecki M. (Ed.), *Mass Transfer. Advancement in Process Modelling*. IntechOpen. DOI: 10.5772/60866.

Almecija M.C., Ibanez R., Guadix A., Guadix E.M., 2007. Effect of pH on the fractionation of whey proteins with a ceramic ultrafiltration membrane. *J. Membr. Sci.*, 288, 28–35. DOI: 10.1016/j.memsci.2006.10.021.

Bai R.B, Leow H.F., 2002. Microfiltration of activated sludge wastewater – The effect of system operation parameters. *Sep. Purif. Technol.*, 29, 189–198. DOI: 10.1016/S1383-5866(02)00075-8.

Brião V.B., Tavares C.R.G., 2012. Pore blocking mechanism for the recovery of milk solids from dairy wastewater by ultrafiltration. *Braz. J. Chem. Eng.*, 29, 393–407. DOI: 10.1590/S0104-66322012000200019.

Casa E.J., Guadix A., Ibanez R., Guadix E.M., 2007. Influence of pH and salt concentration on the cross-flow microfiltration of BSA through a ceramic membrane. *Biochem. Eng. J.*, 33, 110–115. DOI: 10.1016/j.bej.2006.09.009.

Cheang B., Zydney A.L., 2003. Separation of alpha-lactalbumin and beta-lactoglobulin using membrane ultrafiltration. *Biotechnol. Bioeng.*, 83, 201–9. DOI: 10.1002/bit.10659.

Cheng T.W., Wu J.G., 2001. Modified boundary layer resistance model for membrane ultrafiltration. *Tamkang J. Sci. Eng.*, 4 (2), 111–117.

Cinta M., Velaa V., Alvarez Blancoa S., Ja Garcıaa J.L., Bergantinos Rodrıguez E., 2008. Analysis of membrane pore blocking models applied to the ultrafiltration of PEG. *Sep. Purif. Technol.*, 62, 489–498. DOI: 10.1016/j.seppur.2008.02.028.

Dabestani S., Arcot J., Chen V., 2017. Protein recovery from potato processing water: Pre-treatment and membrane fouling minimization. *J. Food Eng.*, 195, 85–96. DOI: 10.1016/j.jfoodeng.2016.09.013.

Ehsani N., Nystrom M., 1995. Fractionation of BSA and myoglobin with modified and unmodified ultrafiltration membranes. *Bioseparation*, 5 (1), 1–10.

Fang Y., 2013. *Study of the effect of surface morphology on mass transfer and fouling behaviour of reverse osmosis and nanofiltration membrane processes.* University of Central Florida, Orlando, Florida. Available at: http://etd.fcla.edu/CF/CFE0004837/Yuming_disseration_final_draft.pdf.

Gkotsis P.K., Banti D.CH., Efrosini N.P., Zouboulis A.I. and Samaras P.E., 2014. Fouling issues in membrane bioreactors (MBRs) for wastewater treatment: Major mechanisms, prevention and control strategies. *Processes*, 2, 795–866. DOI: 10.3390/pr2040795.

Kuca M., Szaniawska D., 2009. Application of microfiltration and ceramic membranes for treatment of salted aqueous effluents from fish processing. *Desalination*, 241, 227–235. DOI: 10.1016/j.desal.2008.01.068.

Lee J., Jeong S., Ye Y., Chen V., Vigneswaran S., Leiknes T., Liu Z., 2016. Protein fouling in carbon nanotubes enhanced ultrafiltration membrane: fouling mechanism as a function of pH and ionic strength. *Sep. Purif. Technol.*, 176, 323–334. DOI: 10.1016/j.seppur.2016.10.061.

Lieu Le N., Nunes S.P., 2016. Materials and membrane technologies for water and energy sustainability. *Sust. Mat. Technol.*, 7, 1–28. DOI:10.1016/j.susmat.2016.02.001.

Lim A.L., Bai R., 2003. Membrane fouling and cleaning in microfiltration of activated sludge wastewater. *J. Membr. Sci.*, 216, 279–290. DOI: 10.1016/S0376-7388(03)00083-8.

Luján-Facundo M.J., Mendoza-Roca J.A., Cuartas-Uribe B., Álvarez-Blanco S., 2015. Evaluation of cleaning efficiency of ultrafiltration membranes fouled by BSA using FTIR–ATR as a tool. *J. Food Eng.*, 163, 1–8. DOI: 10.1016/j.jfoodeng.2015.04.015.

Ma B., Hu C., Wang X., Xie Y., Jefferson W.A., Liu H., Qu J., 2015. Effect of aluminum speciation on ultrafiltration membrane fouling by low dose aluminum coagulation with bovine serum albumin (BSA). *J. Membr. Sci.*, 492, 88–94. DOI: 10.1016/j.memsci.2015.05.043.

Mohammadi T., Kazemimoghadam M., Saadabadi M., 2003. Modeling of membrane fouling and flux decline in reverse osmosis during separation of oil in water emulsions. *Desalination*, 157, 369–375. DOI: 10.1016/S0011-9164(03)00419-3.

Riffat R., 2012. *Fundamental of wastewater treatment and engineering.* CRC Press, 359.

Saxena A., Tripathi B.P., Kumar M., Shahi V.K., 2009. Membrane-based techniques for the separation and purification of proteins: An overview. *Adv. Colloid Interface Sci.*, 145, 1–22. DOI: 10.1016/j.cis.2008.07.004.

Shah T.N., Foley H.C., Zydney A.L., 2007. Development and characterization of nanoporous carbon membranes for protein ultrafiltration. *J. Membr. Sci.*, 295, 40–4. DOI: 10.1016/j.memsci.2007.02.030.

United States Environmental Protection Agency, 2005. *Membrane Filtration Guidance Manual. Office of Water* (4601). EPA815-R-06-009.

Wiesner M.R., Veerapaneni S., Brejchova D.,1992. Improvement in microfiltration using coagulation pretreatment, In: Klute R., Hahn H.H., (Eds.), *Proceedings of the Fifth Gothenburg Symposiumon Chemical Water and Wastewater Treatment II*. Springer, Nice, France, New York, 20–40.

Zulkali M. D., Ahmad A.L., Derek C.J., 2005, Preliminary studies on the effect of pH, ionic strenghtband pressure on protein fractionation. *Desalination*, 179, 381–390. DOI: 10.1016/j.desal.2004.11.084.

Received 05 April 2017
Received in revised form 20 April 2018
Accepted 25 April 2018